HHS Public Access

Author manuscript

ACS Infect Dis. Author manuscript; available in PMC 2019 May 22.

Published in final edited form as:

ACS Infect Dis. 2018 January 12; 4(1): 59–67. doi:10.1021/acsinfecdis.7b00105.

Marine Mammal Microbiota Yields Novel Antibiotic with Potent Activity Against *Clostridium difficile*

Jessica L. Ochoa[1], **Laura M. Sanchez**[1,2], **Byoung-Mo Koo**[3], **Jennifer S. Doherty**[3], **Manohary Rajendram**[4], **Kerwyn Casey Huang**[4,5], **Carol A. Gross**[3], and **Roger G. Linington**[1,6,*]

[1]Department of Chemistry and Biochemistry, University of California Santa Cruz, 1156 High Street, Santa Cruz, CA 95064, USA

[2]Department of Medicinal Chemistry and Pharmacognosy, University ofIllinois at Chicago, 833 South Wood Street, Chicago, H 60612, USA

[3]Department of Microbiology and Immunology, University of California, San Francisco, 513 Parnassus Avenue, San Francisco, CA 94158, USA

[4]Department of Bioengineering, Stanford University, 443 Via Ortega, Stanford, CA 94305, USA

[5]Department of Microbiology and Immunology, Stanford University School ofMedicine, 299 Campus Drive, Stanford, CA 94305, USA

[6]Department of Chemistry, Simon Fraser University, 8888 University Drive, Burnaby, BC V5A 1S6, Canada

Abstract

The recent explosion of research on the microbiota has highlighted the important interplay between commensal microorganisms and the health of their cognate hosts. Metabolites isolated from commensal bacteria have been demonstrated to possess a range of antimicrobial activities, and it is widely believed that some of these metabolites modulate host behavior, affecting predisposition to disease and pathogen invasion. Our access to the local marine mammal stranding network (MMSN) and previous successes in mining the fish microbiota poised us to test the hypothesis that the marine mammal microbiota is a novel source of commensal bacteria-produced bioactive metabolites. Examination of intestinal contents from five marine mammals led to the identification of a *Micromonospora* strain with potent and selective activity against a panel of

*Corresponding author. rliningt@sfu.ca.

Author Contributions

Design and oversight of the project R.G.L., J.L.O.; collection ofbacterial samples and molecular networking J.L.O., L.M.S.; bacterial isolation, antibacterial screening, compound isolation, structure elucidation and flow cytometry J.L.O., non-essential gene library screening B.M.K., J.S.D., C.A.G.; single cell imaging M.R., K.C.H. All authors discussed and commented on the manuscript.

Supporting Information

Phylogenetic tree, molecular networking, structure elucidation (descriptions, figures, and spectra), cytological profiling, flow cytometry, genetic screening data, PI staining images, necroscopy details, sequencing data and organism nomenclature, MIC values for pH and cation dependency.

Conflict of Interest

There are no competing interests.

Data and materials availability: LC-MS/MS data are publicly accessible under MassIVE accession no. MSV000080606, or can be accessed at http://gnps.ucsd.edu/ProteoSAFe/status.jsp?task=e789cd8fbal54737b819994cfl281cfa# DNA sequences have been deposited to GenBank with accession numbers KY580789-KY580816

Gram-positive pathogens and no discernable human cytotoxicity. Compound isolation afforded a new complex glycosylated polyketide, phocoenamicin, with potent activity against the intestinal pathogen *Clostridium difficile*, an organism challenging to treat in hospital settings. Use of our activity-profiling platform, BioMAP, clustered this metabolite with other known ionophore antibiotics. Fluorescence imaging and flow cytometry confirmed that phocoenamicin is capable of shifting membrane potential without damaging membrane integrity. Thus, exploration of gut microbiota in hosts from diverse environments can serve as a powerful strategy for the discovery of novel antibiotics against human pathogens.

Graphical Abstract

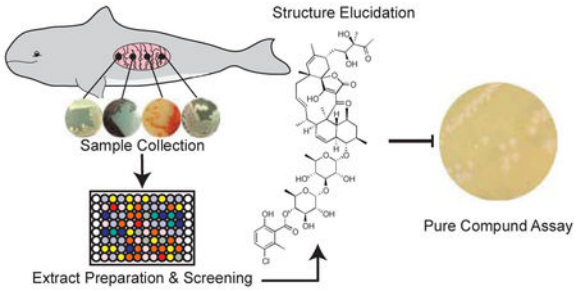

Keywords

microbiome; drug discovery; natural products; porpoise; cytological profiling

With the growing understanding of the complex interplay between microbes and host organisms has come an increased realization that secondary metabolites produced by these microorganisms can modulate host health and behavior.[1–3] Traditionally, investigation of microbial secondary metabolites has been performed on soil-derived isolates that lack a cognate host. In some cases, studies have explored endo-and exosymbionts of several invertebrates.[4–7] However, to date there has been little study of the natural products producing capabilities ofisolates from the microbiota of higher organisms. This study aims to examine isolates from marine mammal microbiota as sources of novel bioactive natural products with activity against clinically relevant human pathogens.

The inception of the Human Microbiome Project in the United States and similar programs in Europe and the rest of the world has led to a dramatic increase in the number of studies aimed at identifying biologically relevant secondary metabolites from microbiome-derived isolates.[8–9] Although the approaches used vary from genome mining[8,10] to ecologically driven discovery,[11] the aim in most cases has been to isolate and characterize secondary metabolites predicted to be connected to the progression or inhibition ofhuman disease. The use of the human microbiome as a source of inspiration for therapeutic development raises important ethical questions. In cases where novel natural products from human microbiota are found to be both protective and highly prevalent, their development into industrially produced bioactive agents brings with it the risk of increased antibiotic resistance. Misuse of these compounds through over-prescription or extended agricultural deployment could create a situation where resistance becomes widespread in the environment, disrupting the

delicate balance between commensal members of the microbiome population and opportunistic pathogens. Therefore, additional methods are needed to address the lack of novel antibiotic candidates currently in development, without creating new resistance liabilities.

An alternative approach to microbiome-inspired natural product discovery is the exploration of isolates from other vertebrates. In contrast to plants and invertebrates, vertebrate-derived microorganisms have not been well studied for natural products production. We hypothesized that, given that vertebrates are frequently challenged with pathogens similar or identical to those that impact human health, vertebrate microbiota may contain biosynthetic genes responsible for the production of novel natural products against these high priority targets. Recent studies in this area support this hypothesis; sampling of roadkill carcasses in Oklahoma[12] yielded a library of 3,659 bacterial isolates, one of which produced a family of four novel lipopeptides with anti-biofilm activities against *Candida albicans*. Additionally, several studies have explored the natural products producing capacity of bacterial isolates from fish intestinal microbiome samples. Our own work in this area has demonstrated the production of bioactive lipids and bile acids from fish microbiome isolates,[13,14] while a separate study by Domig and coworkers led to the isolation of a library of Actinomycetales with diverse antibacterial activities and biosynthetic capacities.[15]

As an extension of our previous studies examining natural products from the fish microbiome we elected to explore the intestinal microbiota of marine mammals for the production of bioactive natural products through our connection with the Monterey Bay Marine Mammal Stranding Network necropsy program. Marine mammals with extensive global migration patterns are exposed to drastic changes in the environment and also possess increased diversity in microbial community structure compared with non-migratory species.[16,17] Interestingly, 70% of the near full-length sequences obtained from cetaceans were significantly distinct by 16S rRNA sequencing compared to published sequences in the NCBI database,[18] indicating that these animals possess unique microbial community structures. To date, the majority of marine mammal microbiome studies have focused on the detection and analysis of pathogens, rather than characterization of their commensal bacteria.[19–22] These surveys have identified a wide array ofbacterial pathogens that are also important in human disease, such as *Pseudomonas aeruginosa* and *Staphylococcus aureus* (including MRSA),[20] suggesting that marine mammals face similar infection risks to humans. Sampling the intestinal microbiota of four different marine mammal species (harbor porpoise, harbor seal, California sea lion and common dolphin) led to the creation of a library ofbacterial isolates that were evaluated for their antibiotic properties against a panel of pathogenic bacteria. From these, one isolate was selected for detailed chemical investigation, resulting in the discovery of phocoenamicin, a novel spirotetronate antibiotic with potent activity against MRSA and *C. difficile*.

Results and Discussion

Sample Collection and Isolate Prioritization for Novel Bioactives Discovery

Samples were collected from five marine mammal carcasses, and bacterial strains isolated, extracted, and prioritized for the identification of small molecule antibiotics (Fig. 1). In

collaboration with the Long Marine Laboratory Marine Mammal Stranding Network (MMSN) located in Santa Cruz, samples of intestinal contents from the carcasses of five marine mammals (harbor porpoise (MMA), harbor seal (MMB), California sea lion (MMC), infant harbor porpoise (MMD), and infant dolphin (MME)) were sampled for their culturable microbiota (Table S1). No visible signs of decomposition were observed and all mammals possessed intact soft tissue such as eyes and fat pads indicating that the mammals were all freshly deceased. From the MMA samples, 48 isolates were obtained using lean isolation media designed to enhance for Actinobacteria. Of these, 28 were selected for further sequencing analysis (Fig. S1). 16S rRNA sequencing showed that the majority (22/28) of the sequenced bacteria were Firmicutes, while Actinobacteria comprised 21.4% (Table S2). The lowest sequence identity observed in comparison with published strains was 94.4% with a *Bacillus oceanisediminis* strain. To prioritize organisms for chemical evaluation, we selected strains with low sequence identity to published strains, as well as strains from genera considered understudied in terms of Actinobacterial natural products production, such as *Micromonospora*.

Metabolites from colonies grown on agar plates were also extracted with organic solvents and analyzed by direct infusion tandem mass spectrometry. A molecular network was assembled based on the fragmentation patterns of the extracted metabolites produced from those colonies, 23 using Global Natural Products Social molecular networking (GNPS) (Fig. S2).[23] Metabolites were characterized as unique if they were produced by only a single organism. The five organisms within the sample set that displayed the highest number of unique metabolites were also prioritized. In total, eleven organisms were fermented at large scale, extracted, and fractionated for biological screening.

Biological Screening of Crude Extracts Reveals Potent Activity Against Gram-Positive Bacteria

To determine the effectiveness of the metabolite fractions, we performed high-throughput screening against a panel of 15 BLS1 and BSL2 pathogens using our in-house BioMAP assay, which clusters antibiotic compounds based on their activity profiles across the test panel.[24] These data indicated that seven of the eleven prioritized organisms possessed antimicrobial activity against at least one bacterial strain (Fig. 2). This hit rate is comparable to our traditional library of non-marine mammal-associated bacteria, where approximately half of allstrains show some degree of antibacterial activity against one or more test strains. Secondary screening of dilution series of active fractions (16 two-fold dilutions) highlighted fraction RLFI1036F from *Micromonospora auratinigra* as a high potency lead, with activity against Gram-positive bacteria down to the lowest tested concentration (Fig. 2). This fraction was therefore prioritized for further analysis utilizing our standard natural product isolation protocol. After two stages of fractionation, we were able to isolate a single bioactive component possessing mass spectrometric *mlz* features of 1071.4 and 1093.4, consistent with the $[M+H]^+$ and $[M+Na]^+$ adducts for a molecule with a mass of 1070.4 Da.

Structure Elucidation of a Novel Natural Product, Phocoenamicin

Evaluation of the high-resolution mass spectrometry (HRMS) *mlz* value for the precursor ion, coupled with examination of the isotopic distribution, suggested a molecular formula of

$C_{56}H_{75}ClO_{18}$. The planar structure was assembled by NMR analysis, using a combination of ^{1}H, ^{13}C, gCOSY, gHSQC, gHMBC, and TOCSY spectra (Fig. 3A). Extensive exploration of crystallization conditions for single crystal X-ray diffraction proved unsuccessful, as has been the case for a number of other spirotetronate natural products.[25] However, determination of the configuration for all 23 stereogenic centers in phocoenamicin was accomplished using a combination of spectroscopic and chemical derivatization methods; the constitution and relative configuration of the polyketide core of the molecule were determined using NMR methods, while the carbohydrate monomers were determined using a combination of NMR analyses and degradation and derivatization studies in comparison with commercially available standards.

The aliphatic core was the first subunit to be assembled, from C3 to C17. Beginning with methylene protons H17α and H17β, COSY correlations revealed a long linear spin system comprising eleven contiguous protonated carbons (subunit B1, Fig. S3). HSQC and HMBC correlations confirmed these assignments, and revealed the presence of an additional subunit comprising seven carbons (C3 to C7, subunit B2, Fig. S3). These two subunits were connected through key HMBC correlations from H25 to C13 and from H27 to the methylene carbon at C7. Additional HMBC correlations identified a decalin core ring structure via HMBC correlations from H5 to both C9 and C10.

Next, the cyclohexene unit (C18 to C23) was identified, starting from olefinic proton H19 (Fig. S3). A strong HMBC correlation from H19 to a quaternary olefinic carbon (C20) suggested the presence of a tri-substituted olefin. HMBC correlations from a singlet methyl at δH 1.72 (H30) to both olefinic carbons indicated a vinylic methyl substitution on C20, which was confirmed by a reciprocal HMBC correlation from olefinic proton H19 to methyl carbon C30. This subunit was extended through a combination ofHMBC, COSY, and TOCSY correlations to give a five-carbon chain from C19 to C32, which was connected to tertiary alcohol C33 via an HMBC correlation from the methyl protons on H36 and to carbon C32 and C33. This subunit was further extended via HMBC correlations from methyl protons on H36 to carbonyl carbon C34. This carbonyl belonged to a small terminal subunit comprised of a diagnostic sharp methyl ketone singlet at δH 2.21, δC 24.8 (C35). Finally, HMBC correlations between methyl protons H29 and carbons C19 and C23, in conjunction with HMBC correlations between methylene protons H22 and C23 closed this subunit as a cyclohexene with a diol sidechain. Reciprocal HMBC correlations between C29 and C17 allowed the connection of the cyclohexene unit to the aliphatic core through the bond between C17 and C18. Finally, the planar structures of the two hexose moieties and the terminal chlorophenol were determined using standard methods (Supporting information).

To complete the assignment of the planar structure of this new metabolite we examined key hetereonuclear correlations between the identified subunits. Reciprocal HMBC correlations between the oxygenated methine at C9 on the decalin unit and the anomeric position at Cl' on the glycosidic sidechain revealed an ether linkage between these two motifs, completing the assembly of all the major fragments. With this extended fragment in place, consideration of the molecular formula indicated the absence of atoms C_3HO_2 and four double bond equivalents (DBEs). Comparison of this late-stage partial structure with the existing literature revealed a number of other molecules with similar core motifs.[25] Common to these

structures is a central tetronic acid motif that was internally consistent with the remaining atoms for phocoenamicin. A HMBC correlation from H17 to C23 corroborated the presence of the spirocenter in the tetronic acid, which was further confirmed by consideration of the ^{13}C chemical shifts for this final structural element, which were in good alignment with literature values. Installation of this functional group completed the planar structural assignment (Figure 3A), and accounted for all atoms and DBEs indicated form the molecular formula.

The relative configuration of phocoenamicin was established through a combination of ROESY correlations and ^{1}H-^{1}H coupling constants beginning with the decalin core to define all chiral centers in this 6–6 fused ring system. A key ROE between H13 and H15 defined H15 on the bottom face of the molecule. A large $^{3}J_{HH}$ coupling constant (15 Hz) between H15 and H16 assigned the 0lef1n as *trans*. Examination of the ROE correlations for H15 to methyl C28 and H16 to C29 defined these two methyl groups as located on the bottom and top face, respectively. A coupling constant of 10.8 Hz between H16 and H17α indicated that they were on opposite faces. A coupling constant of 2.4 Hz between H16 and H17β demonstrated that they were both on the top face. ROE correlations between C29 to H22α in addition to a ROE between H21 and H22α assigned H21 to the top face. Examination of the DQF-COSY and lD-TOCSY revealed a coupling constant of 7.4 Hz between H21 and H22β, and a coupling constant <3 Hz between H21 and H22α which reaffirmed that H21 and H22α were on the top face.

The most challenging component of structure elucidation was the configurational assignment of the diol sidechain (C31 to C35). Extensive signal overlap in the proton NMR spectrum precluded the facile extraction of coupling constants for this key region. Application of a selective lD TOCSY experiment irradiating the proton at δH 2.45 (C21) on the bridgehead of the alkyl chain, in conjunction with data derived from a DQF-COSY spectrum in this region, provided clear evidence for the coupling constants associated with H21, H31 and H32.

For the methylene at C31, a large coupling constant of 9.6 Hz was observed between H31α and the adjacent proton H21, suggesting an approximate dihedral angle of either 0° or 180°. A small coupling constant of 3.1 Hz between H21 and H31β indicated a *gauche* relationship. Taken together, these coupling constants suggested the atom arrangement depicted in Fig. 3B. This arrangement was further confirmed by the presence of reciprocal ROE correlations between the H21 and H31β. Extending along the sidechain, H31α possessed a medium-sized coupling constant (4.8 Hz) to the adjacent proton H32, with corresponding ROE correlations indicating a *gauche* relationship. Additionally, a large coupling constant (10.2 Hz) between H32 and H31β indicated an *anti* relationship (Fig. 3C). Considering the above correlations, all four diastereomers were built and modeled in Discovery Studio 4.0. Diastereomers possessing the (*S*) configuration at C33 or the (*R*) configuration at C32 exhibited conformers that compromised at least one observed ROE correlation in each conformation (Fig. S4). Only one diastereomer (32*S*, 33*R)* aligned with all the observed ROE correlations, setting the final bond orientation (Fig. 3D) and completing the full relative configurational analysis of the polyketide portion. While a *J*-resolved HMBC was inconclusive due to overlapped signals, based on the biosynthesis of this class of molecules,

it was hypothesized that the tetronic acid stereogenic center should be assigned a *(S*)* configuration in alignment with other members in this class.[25] Absolute, and relative confirmation of the carbohydrates was achieved by NMR, degradation studies and comparison with standards (Supporting information). These analyses revealed a novel spirotetronate macrocyclic core with a carbon skeleton containing 23 chiral centers that we named phocoenamicin after the harbor porpoise genus *Phocoena* (Fig. 4).

Phocoenamicin possesses potent activity against *Clostridium difficile*

BioMAP screening of phocoenamicin against a panel of clinically relevant bacteria revealed potent activity against our panel of Gram-positive bacteria (Table 1). Comparison of phocoenamicin to other structures within the spirotetronate class revealed that, while phocoenamicin shares a similar macrolide backbone to maklamicin and an aromatic appendage to chlorothricin (Fig. 4),), it possesses several unique structural features including the diol sidechain and the presence of two 6-deoxy sugars that are unusual within this class. Several compounds in this class possess antimicrobial activity against Gram-positive bacteria and tumor cells, with previous analysis indicating hydroxylation and glycosylation patterns have dramatic effects on biological attributes of this compound class.[25,26]

Within the spirotetronate class, decatromicin B, produced from *Actinomadura* sp. 2EPS, displays potent activity against *Clostridium difficile*,[27] an antibiotic-associated pathogen that causes ç500,000 infections and is linked to >29,000 deaths per year.[28] Decatromicin B possesses a larger macrocyclic core than phocoenamicin but contains a similar chlorinated aromatic subunit attached to the macrocyclic core via a sugar linkage. This feature is observed in both phocoenamicin and fidaxomicin (Fig. 4), a promising narrow spectrum antibiotic for treating *C.difficile* infections. Both phocoenamicin and fidaxomicin possess a 6-deoxy sugar with an acetyl linkage to a chlorinated phenol, prompting us to evaluate phocoenamicin against *C. difficile*. Limited information is available on mortality rates of marine mammals from *C. difficile* infections, however *Clostridium* species are relevant to cetaceans and have been isolated from intestinal and fecal samples from dolphins and whales.[19,29] An emerging threat to humans, this pathogen has limited treatment options, with current therapy consisting of an aggressive dosage of vancomycin and/or fecal transplants to try to re-establish microbiome health.[30] Screening of phocoenamicin against *C. difficile* (ATCC 700057) according to CSLI guidelines revealed comparable activity (MIC: 2.6 μM) to vancomycin (MIC: 2.9 μM).[31]

Biological activity of phocoenamicin mimics ionophores

A distantly related spirotetronate, spirohexenolide A (Fig. 4), has previously been analyzed in a bacterial cytological profiling assay which revealed that it rapidly permeabilized cells resulting in the collapse of the proton motive force.[32] Observation of spirohexenolide A in tumor cells revealed the binding to and modulation of human macrophage migration inhibitor factor.[33] To examine whether phocoenamicin impacted mammalian cell development, we employed our image-based cytological profiling platform (Fig. 5A).[34,35] HeLa cells remained viable after 24 h of incubation with phocoenamicin, with only the two highest concentrations (73 and 146 μM) showing subtle changes in cell morphology (Fig. 5B). At these concentrations, phocoenamicin clustered with known ionophores and

mitochondrial decouplers, suggesting that the mechanism of action (MOA) is related to modification ofionic gradients across the cell membrane (Fig. 5C). To further probe the MOA, we screened a *Bacillus subtilis* essential gene knockdown (CRISPRi) library and transposon-insertion library against phocoenamicin (Fig. S11A). Previous studies have demonstrated that chemical screening against genome-wide libraries is an effective platform for the discovery of drug targets.[36,37] As expected, strains over-producing multidrug efflux pumps (Mdt) were identified as phocoenamicin-resistant (up to 4x MIC). However, we were not able to identify a direct target of phocoenamicin from either the CRISPRi or transposon-insertion library (Fig. S11B). Thus, these results also support the idea that the target of phocoenamicin, rather than being a protein, might be an essential cellular function, such as the transmembrane ionic gradients suggested by cytological profiling.

For other ionophores, varying calcium or magnesium concentration, or altering the pH of the growth medium can have drastic effects on potency.[38] However, when we systematically changed these variables in our growth medium, we did not observe a significant effect on the MIC of phocoenamicin against *S. aureus* (Table S4). Thus, calcium does not induce conformational changes that affect phocoenamicin bioactivity, as proposed for daptomycin, a calcium-dependent antimicrobial that is active against Gram-positive bacteria.[39] Gram-positive bacteria such as *S. aureus* and *C. difficile* can survive in acidic environments through a variety of mechanisms such as changes to membrane composition and proton pumps.[40] These defense mechanisms can also make them resistant to antibiotics; nonetheless, our results indicated that phocoenamicin retains its chemical stability and potency against *S. aureus* in acidic conditions. Considering both the BioMAP and cytological profiling, we performed fluorescence-activated cell sorting (FACS) to evaluate phocoenamicin as an ionophore in *S. aureus*. We determined that phocoenamicin has the ability to effectively depolarize the membrane when compared to the positive control carbonyl cyanide w-chlorophenyl hydrazone (Fig. S10).[41] To determine whether phocoenamicin permeabilizes the membrane in a similar manner to spirohexenolide A, we monitored propidium iodide (PI) fluorescence directly after treatment with 0.5X MIC phocoenamicin in a microfluidic perfusion system (Methods). As expected, cells treated with ethanol exhibited bright PI staining after 10 min. By contrast, PI staining remained essentially unchanged even 20 min after treatment with phocoenamicin or DMSO. Thus, phocoenamicin likely disrupts membrane potential without affecting membrane integrity.

Conclusion

Unique access to the Marine Mammal Stranding Network allowed us to explore several marine mammal microbiotas. Isolation of 48 culturable microorganisms from an otherwise healthy harbor porpoise prior to stranding, combined with biological assays, showed the antimicrobial potential of microbiota-based collections. Limited information is available about the compounds produced by mammalian bacterial isolates, or the likely endogenous roles of those compounds. Prioritization of *Micromonospora auratinigra* from the harbor porpoise microbiota revealed the presence of a new glycosylated polyketide antibiotic, phocoenamicin, with potent activity against a broad panel of Gram-positive organisms including the intestinal pathogen *C. difficile*. The discovery of phocoenamicin has

highlighted the potential of marine mammal commensal microbes for drug discovery and host protection.

Phocoenamicin possesses comparable activity to vancomycin, the current frontline antibiotic against *C. difficile* infections. Interrogation of the MOA for phocoenamicin using a suite of approaches demonstrated that phocoenamicin functions by disrupting membrane potential without affecting membrane integrity. Vancomycin has previously been shown to have no impact on membrane potential,[42] suggesting disparate MOAs for these two compounds. A second emerging treatment for *C. difficile*, fidaxomicin, shares several similar structural features with phocoenamicin. Although both phocoenamicin and fidaxomicin have stable MICs across varying cation and pH conditions, lack of sensitivity of an RNA polymerase knock-down strain in *B. subtilis* suggests that phocoenamicin possesses a different mechanism of action to fidaxomicin, which has been shown to target RNA polymerase.[43] Together these results suggest phocoenamicin functions by an alternative mechanism to any of the existing treatments for *C. difficile* used in clinical practice. The discovery of this novel spirotetronate antibiotic demonstrates the value in exploring niche microbiota environments for novel compound discovery, and provides incentive for further investigation of the understudied host-microbe environment of marine mammals.

Materials and Methods

General Experimental Procedures

Chromatography solvents were HPLC-grade, and were used without further purification. Optical rotations were measured on a Jasco P-2000 polarimeter using a 10-mm path length cell at 589 nm. UV spectra were recorded on a Shimadzu UV-visible spectrophotometer (UV-1800) with a path length of 1 cm. NMR spectra were acquired on a Varian Inova 600-MHz spectrometer equipped with a 5 mm H/C/N triple resonance cryoprobe and referenced to residual solvent proton and carbon signals (δ_H 2.05, δ_c 29.84, for acetone-d6 and δ_H 7.26, δ_c 77.16 for chloroform-d). HRMS data were acquired using an Agilent 6230 electrospray ionization accurate-mass time-of-flight liquid chromatograph mass spectrometer.

Cultivation of Bacteria

Marine mammal intestinal contents were transferred to sterile Falcon tubes, 1 mL of sterile Milli-Q water was added, and the samples were vortexed for 1 min. Four solid agar media were used for microbial isolation: actinomycete isolation agar (Difco), SNS, and modified NTS and HVS.[13,14] All isolation plates were prepared with sterile sea water and supplemented with 50 mg/L of both cyclohexamide and nalidixic acid. Intestinal contents were plated using three different methods: 1) the mixture was serially stamped onto solid agar with a sterile swab, 2) the mixture was diluted with 1 mL of sterile Milli Q water and 100 μL of the resulting mixture was spread onto the plate surface, and 3) the mixture was diluted with 10 mL of sterile Milli-Q water and 100 μL of the resulting mixture was spread onto the plate surface. Cultures were incubated at room temperature and bacterial colonies displaying desired morphologies were subcultured on Difco Marine Broth solid agar plates until pure. Typical incubation times for the appearance of colonies from isolation plates ranged from 30–90 days.

DNA Isolation, PCR Amplification, and Sequencing

Genomic DNA was extracted using the Wizard® Genomic DNA Purification Kit (Promega) by picking a single colony of the cultured strains according to manufacturer's instructions. For PCR amplification of the 16S rRNA gene, the primer pair 8F (5'-AGAGTTTGATCCTGGCTCAG-3') and 1492R (5'-GGTTACCTTGTTACGACTT-3') was used. Platinum® Taq DNA Polymerase, High Fidelity (Invitrogen) was used for amplification according to manufacturing protocol Pub. No. MAN0000948 Rev. A.0 to achieve a total reaction volume of 25 μL. PCR was performed on an Eppendorf Mastercycler Personal thermocycler under the following conditions: initial denaturation 95°C for 5 min, 35 cycles of denaturation at 95°C for 1 min, annealing at 50°C for 1 min, extension at 72°C for 90 s, and a final extension at 72°C for 10 min. After confirmation by gel electrophoresis (1% agarose gel in IX TAE buffer), the PCR products were purified with QIAQuick PCR Purification Kit (Qiagen) and sent to Sequetech Corporation for sequencing using the same PCR primers described above plus an additional middle primer 341F (5'-CCTACGGGAGGCAGCAG-3'). DNA sequences have been deposited to GenBank with accession numbers KY580789-KY580816.

Single-cell imaging

Imaging was performed on a Ti-E Eclipse microscope (Nikon Instruments, Inc., Melville, NY, USA) with a 1.4NA 100X objective. Images were acquired with an Andor DU885 (Andor Technology, South Windsor, CT, USA) camera, using μManager v. 1.4.[44] Temperature was maintained within a custom environmental chamber (HaisonTech, Taipei, Taiwan). To measure cell permeability after treatment, cells were loaded into a B04 bacterial microfluidic chip in a CellASIC ONIX system (EMD Millipore, Hayward, CA, USA) and propidium iodide fluorescence was monitored every 1 min.

Molecular Networking

Bacteria were extracted, then directly infused into the mass spectrometer using a Triversa nanomate-electrospray ionization source (Advion Biosystems) coupled to a 6.42 T Thermo LTQ-FT-ICR mass spectrometer. Briefly, bacterial colony plugs were extracted with 100 μL of 50:50 $MeOH_2O$ and 100 μL of butanol for 1 h at room temperature. Following this extraction, samples were centrifuged at 10,000 rpm for 2 min and 10 μL was diluted into 1 mL of 50:50 ACN:H_20. This solution was centrifuged at 10,000 rpm for 2 min and diluted another 10-fold, then directly infused using a back pressure of 0.35–0.5 psi and a spray voltage of 1.3–1.45 kV. FT-MS and ion trap MS/MS spectra were acquired using Tune Plus software v. 1.0 and Xcalibur software v. 1.4 SR1. The instrument was tuned on *m/z* 816, the 15+ charge state of cytochrome C. The instrument scan cycle consisted of one 10-min segment, during which a profile FT scan with a resolution of 25,000 was cycled with four data-dependent scans in the ion trap. The data-dependent scan iteratively cycled through the top four most intense ions from the FT scan, after which they were placed on an exclusion list for 600 s. Data was converted using MSConvert (Proteowizard) to 32-bit mzXML with peak picking level 1.

A molecular network was created using the online workflow at GNPS. The data was then clustered with MS-Cluster with a parent mass tolerance of 1.0 Da and a MS/MS fragment

ion tolerance of 0.3 Da to create consensus spectra. A network was then created where edges were filtered to have a cosine score above 0.5 and more than 6 matched peaks. Further edges between two nodes were kept in the network if and only if each of the nodes appeared in each other's respective top 10 most similar nodes.

Supplementary Material

Refer to Web version on PubMed Central for supplementary material.

Acknowledgments

The authors thank Vicki Auerbuch Stone for providing BSL2 space to culture *C. difficile*, Robin Dunkin for performing the necroscopies, Bari Holm Nazario for assistance with flow cytometry analysis, Walter Bray and Scott Lokey for access to the UCSC chemical screening center, Jack Lee for assistance with NMR spectroscopy, and NOAA for permitting us to access the intestinal samples for analysis. We thank Pieter Dorrestein at The Collaborative Mass Spectrometry Innovation Center at the UCSD School ofPharmacy for assistance with molecular networking and GNPS analyses.

Funding: Funding was provided in part by a UCSC Cota-Robles predoctoral fellowship (to J.L.O.), NSF CAREER Award MCB-1149328 (to K.C.H.), the Allen Discovery Center for Multiscale Systems Modeling ofMacrophage Infection (to M.R. and K.C.H.), a NSF GRFP (to L.M.S.), UIC Startup Funds (to L.M.S.), and Natural Sciences and Engineering Research Council of Canada Grant RGPIN-2016–03962 (to R.G.L.)

References and Notes

(1). Turroni S, Brigidi P, Cavalli A, and Candela M (2017) Microbiota-Host Transgenomic Metabolism, Bioactive Molecules from the Inside. J.Med. Chem DOI: 10.1021-acs.jmedchem. 7b00244.

(2). Donia MS, and Fischbach MA (2015) HUMAN MICROBIOTA. Small molecules from the human microbiota. Science 349, 1254766. [PubMed: 26206939]

(3). Nepelska M, de Wouters T, Jacouton E, Béguet-Crespel F, Lapaque N, Doré J, Arulampalam V, and Blottière HM (2017) Commensal gutbacteria modulate phosphorylation-dependent PPARγ transcriptional activity in human intestinal epithelial cells. Sci. Rep 7, 43199. [PubMed: 28266623]

(4). Schneemann I, Nagel K, Kajahn I, Labes A, Wiese J, and Imhoff JF (2010) Comprehensive Investigation ofMarine*Actinobacteria* Associated with the Sponge *Halichondriapanicea*. Appl. Environ. Microbiol 76, 3702–3714. [PubMed: 20382810]

(5). Abdelmohsen UR, Bayer K, and Hentschel U (2014) Diversity, abundance and natural products of marine sponge-associated actinomycetes. Nat. Prod. Rep 31, 381–399. [PubMed: 24496105]

(6). Valliappan K, Sun W, and Li Z (2014) Marine actinobacteria associated with marine organisms and their potentials in producing pharmaceutical natural products. Appl. Microbiol. Biotechnol 98, 7365–7377. [PubMed: 25064352]

(7). Behie SW, Bonet B, Zacharia VM, McClung DJ, and Traxler MF (2016) Molecules to Ecosystems: Actinomycete Natural Products In situ. FrontMicrobiol 7, 2149.

(8). Wilson MR, Zha L, and Balskus EP (2017) Natural product discovery from the human microbiome. J. Biol. Chem 292, 8546–8552. [PubMed: 28389564]

(9). Franzosa EA, Huang K, Meadow JF, Gevers D, Lemon KP, Bohannan BJM, and Huttenhower C (2015) Identifying personal microbiomes using metagenomic codes. Proc. Natl. Acad. Sci 112, E2930–8. [PubMed: 25964341]

(10). Trautman EP, and Crawford JM (2016) Linking Biosynthetic Gene Clusters to their MetabolitesviaPathway-TargetedMolecularNetworking. Curr. Top. Med. Chem 16, 1705–1716. [PubMed: 26456470]

(11). Zipperer A, Konnerth MC, Laux C, Berscheid A, Janek D, Weidenmaier C, Burian M, Schilling NA, Slavetinsky C, Marschal M, Willmann M, Kalbacher H, Schittek B, Brötz-Oesterhelt H,

Grond S, Peschel A, and Krismer B (2016) Human commensals producing a novel antibiotic impair pathogen colonization. Nature 535, 511–516. [PubMed: 27466123]

(12). Motley JL, Stamps BW, Mitchell CA, Thompson AT, Cross J, You J, Powell DR, Stevenson BS, and Cichewicz RH (2017) Opportunistic Sampling ofRoadkill as an Entry Point to Accessing Natural Products Assembled by Bacteria Associated with Nonanthropoidal Mammalian Microbiomes. J.Nat. Prod 80, 598–608. [PubMed: 28335605]

(13). Sanchez LM, Cheng AT, Warner CJA, Townsley L, Peach KC, Navarro G, Shikuma NJ, Bray WM, Riener RM, and Yildiz FH (2016) Biofilm Formation and Detachment in Gram-Negative Pathogens Is Modulated by Select Bile Acids. PLoS ONE e0149603. [PubMed: 26992172]

(14). Sanchez LM, Wong WR, Riener RM, Schulze CJ, and Linington RG (2012) Examining the Fish Microbiome: Vertebrate-Derived Bacteria as an Environmental Niche for the Discovery ofUnique Marine Natural Products. PLoS ONE 7, e35398. [PubMed: 22574119]

(15). Jami M, Ghanbari M, Kneifel W, and Domig KJ (2015) Phylogenetic diversity and biological activity of culturable Actinobacteria isolated from freshwater fish gut microbiota. Microbiol. Res 175, 6–15. [PubMed: 25662514]

(16). Kohl KD, Skopec MM, and Dearing MD (2014) Captivity results in disparate loss of gut microbial diversity in closely related hosts. Conserv. Physiol 2, cou009. [PubMed: 27293630]

(17). Delport TC, Bik EM, Power ML, Costello EK, Harcourt RG, Switzer AD, Webster KN, Callahan BJ, Tetu SG, Holmes SP, Wells RS, Carlin KP, Jensen ED, Venn-Watson S, and Relman DA (2016) Colony Location and Captivity Influence the Gut Microbial Community Composition of the Australian Sea Lion *{Neophoca cinerea)*. Appl. Environ. Microbiol 82, 3440–3449. [PubMed: 27037116]

(18). Bik EM, Costello EK, Switzer AD, Callahan BJ, Holmes SP, Wells RS, Carlin KP, Jensen ED, Venn-Watson S, and Relman DA (2016) Marine mammals harbor unique microbiotas shaped by and yet distinct from the sea. Nat. Commun 7, 10516. [PubMed: 26839246]

(19). Guass 0, Haapanen LM, Dowd SE, Sirovic A, and McLaughlin RW (2016) Analysis of the microbial diversity in faecal material of the endangered blue whale, *Balaenoptera musculus*. Antonie van Leeuwenhoek 109, doi:10.1007-sl0482-016-0698-l.

(20). Higgins R (2000) Bacteria and fungi of marine mammals: a review. Can. Vet. J 41, 105–116. [PubMed: 10723596]

(21). Nelson TM, Rogers TL, and Brown MV (2013) The Gut Bacterial Community of Mammals from Marine and Terrestrial Habitats. PLoS ONE (Gilbert, J. A., Ed.) 8, e83655.

(22). Mootapally CS, Poriya P, Nathani NM, and A VMB (2017) Recent Advances in the Metagenomics ofMarine Mammals Microbiome, in UnderstandingHost-Microbiome Interactions - An OmicsApproach. (Singh RP, Kothari R, Koringa PG, and Singh SP, Eds.). Springer, Singapore.

(23). Wang M, Carver JJ, Phelan VV, Sanchez LM, Garg N, Peng Y, Nguyen DD, Watrous J, Kapono CA, Luzzatto-Knaan T, Porto C, Bouslimani A, Melnik AV, Meehan MJ, Liu W-T, Crüsemann M, Boudreau PD, Esquenazi E, Sandoval-Calderón M, Kersten RD, Pace LA, Quinn RA, Duncan KR, Hsu C-C, Floros DJ, Gavilan RG, Kleigrewe K, Northen T, Dutton RJ, Parrot D, Carlson EE, Aigle B, Michelsen CF, Jelsbak L, Sohlenkamp C, Pevzner P, Edlund A, McLean J, Piel J, Murphy BT, Gerwick L, Liaw C-C, Yang Y-L, Humpf H-U, Maansson M, Keyzers RA, Sims AC, Johnson AR, Sidebottom AM, Sedio BE, Klitgaard A, Larson CB, Boya PCA, Torres-Mendoza D, Gonzalez DJ, Silva DB, Marques LM, Demarque DP, Pociute E, O'Neill EC, Briand E, Helfrich EJN, Granatosky EA, Glukhov E, Ryffel F, Houson H, Mohimani H, Kharbush JJ, Zeng Y, Vorholt JA, Kurita KL, Charusanti P, McPhail KL, Nielsen KF, Vuong L, Elfeki M, Traxler MF, Engene N, Koyama N, Vining OB, Baric R, Silva RR, Mascuch SJ, Tomasi S, Jenkins S, Macherla V, Hoffman T, Agarwal V, Williams PG, Dai J, Neupane R, Gurr J, Rodriguez AMC, Lamsa A, Zhang C, Dorrestein K, Duggan BM, Almaliti J, Allard P-M, Phapale P, Nothias L-F, Alexandrov T, Litaudon M, Wolfender J-L, Kyle JE, Metz T0, Peryea T, Nguyen D-T, VanLeer D, Shinn P, Jadhav A, Müller R, Waters KM, Shi W, Liu X, Zhang L, Knight R, Jensen PR, Palsson B0, Pogliano K, Linington RG, Gutiérrez M, Lopes NP, Gerwick WH, Moore BS, Dorrestein PC, and Bandeira N (2016) Sharing and community curation of mass spectrometry data with Global Natural Products Social MolecularNetworking. Nat. Biotechnol 34, 828–837. [PubMed: 27504778]

(24). Wong WR, Oliver AG, and Linington RG (2012) Development of Antibiotic Activity Profile Screening for the Classification and Discovery ofNatural Product Antibiotics. Chem. Biol 19, 1483–1495. [PubMed: 23177202]

(25). Lacoske MH, and Theodorakis EA (2015) Spirotetronate Polyketides as Leads in Drug Discovery. J.Nat. Prod 78, 562–575. [PubMed: 25434976]

(26). Vieweg L, Reichau S, Schobert R, Leadlay PF, and Süssmuth RD (2014) Recent advances in the field ofbioactive tetronates. Nat. Prod. Rep 31, 1554–1584. [PubMed: 24965099]

(27). Euanorasetr J, Intra B, Mongkol P, Chankhamhaengdecha S, Tuchinda P, Mori M, Shiomi K, Nihira T, and Panbangred W (2015) Spirotetronate antibiotics with anti-*Clostridium* activity from *Actinomadura* sp. 2EPS. WorldJ.Microbiol. Biotechnol 31, 391–398.

(28). Lessa FC, Winston LG, and McDonald LC (2015) Burden of *Clostridium difficile* Infection in the United States. N.Engl. J.Med. 372, 2369–2370. [PubMed: 26061850]

(29). Avalos-Téllez R, Suárez-Güemes F, Carrillo-Casas EM, and Hemandez-Castro R (2010) Bacteria and yeast normal microbiota from respiratory tract and genital area ofbottlenose dolphins (Tursiops truncatus), in CurrentResearch Topics inAppliedMicrobiology and Microbial Biotechnology (Mendez-Vilas A, Ed.) 1st ed., pp 666–673. World Scientific Publishing Company.

(30). van Nood E, Vrieze A, Nieuwdorp M, Fuentes S, Zoetendal EG, de Vos WM, Visser CE, Kuijper EJ, Bartelsman JFWM, Tijssen JGP, Speelman P, Dijkgraaf MGW, and Keller JJ (2013) Duodenal infusion of donor feces for recurrent *Clostridium difficile*. N.Engl. J.Med. 368, 407–415. [PubMed: 23323867]

(31). Wiegand I, Hilpert K, and Hancock REW (2008) Agar and broth dilution methods to determine the minimal inhibitory concentration (MIC) of antimicrobial substances. Nat. Protoc 3, 163–175. [PubMed: 18274517]

(32). Nonejuie P, Burkart M, Pogliano K, and Pogliano J (2013) Bacterial cytological profiling rapidly identifies the cellular pathways targeted by antibacterial molecules. Proc. Natl. Acad. Sci 110, 16169–16174. [PubMed: 24046367]

(33). Yu W-L, Jones BD, Kang M, Hammons JC, La Clair JJ, and Burkart MD (2013) Spirohexenolide A targets human macrophage migration inhibitory factor (hMIF). J. Nat. Prod 76, 817–823. [PubMed: 23659282]

(34). Schulze CJ, Bray WM, Woerhmann MH, Stuart J, Lokey RS, and Linington RG (2013) "Function-First" Lead Discovery: Mode of Action Profiling ofNatural Product Libraries Using Image-Based Screening. Chem. Biol 20, 285–295. [PubMed: 23438757]

(35). Woehrmann MH, Bray WM, Durbin JK, Nisam SC, Michael AK, Glassey E, Stuart JM, and Lokey RS (2013) Large-scale cytological profiling for functional analysis of bioactive compounds. Mo/. BioSyst. 9, 2604–2617.

(36). Peters JM, Colavin A, Shi H, Czamy TL, Larson MH, Wong S, Hawkins JS, Lu CHS, Koo B-M, Marta E, Shiver AL, Whitehead EH, Weissman JS, Brown ED, Qi LS, Huang KC, and Gross CA (2016) A Comprehensive, CRISPR-based Functional Analysis ofEssential Genes in Bacteria. Cell 165, 1493–1506. [PubMed: 27238023]

(37). Wang H, Claveau D, Vaillancourt JP, Roemer T, and Meredith TC (2011) High-frequency transposition for determining antibacterial mode of action. Nat. Chem. Biol 7, 720–729. [PubMed: 21892185]

(38). Chow JM, and Russell JB (1990) Effect ofionophores and pH on growth of *Streptococcus bovis* in batch and continuous culture. Appl. Environ. Microbiol 56, 1588–1593. [PubMed: 2383003]

(39). Micklefield J (2004) Daptomycin Structure and Mechanism of Action Revealed. Chem. Biol 11, 887–888. [PubMed: 15271343]

(40). Cotter PD, and Hill C (2003) Surviving the Acid Test: Responses of Gram-Positive Bacteria to Low pH.Microbiol. Mol. Biol. Rev 67, 429–453. [PubMed: 12966143]

(41). Silverman JA, Perlmutter NG, and Shapiro HM (2003) Correlation ofDaptomycin Bactericidal Activity and Membrane Depolarization in *Staphylococcus aureus*. Antimicrob. Agents Chemother. 47, 2538–2544. [PubMed: 12878516]

(42). Yarlagadda V, Akkapeddi P, Manjunath GB, and Haldar J (2014) Membrane active vancomycin analogues: a strategy to combat bacterial resistance. J.Med. Chem 57, 4558–4568. [PubMed: 24846441]

(43). Goldstein EJC, Babakhani F, and Citron DM (2012) Antimicrobial Activities of Fidaxomicin. Clin. Infect. Dis 55 Suppl 2, S143–8. [PubMed: 22752863]

(44). Edelstein A, Amodaj N, Hoover K, Vale R, and Stuurman N (2010) Computer control of microscopes using μManager. Curr. Protoc. Mol. Biol 92, 14.20:14.20.1–14.20.17.

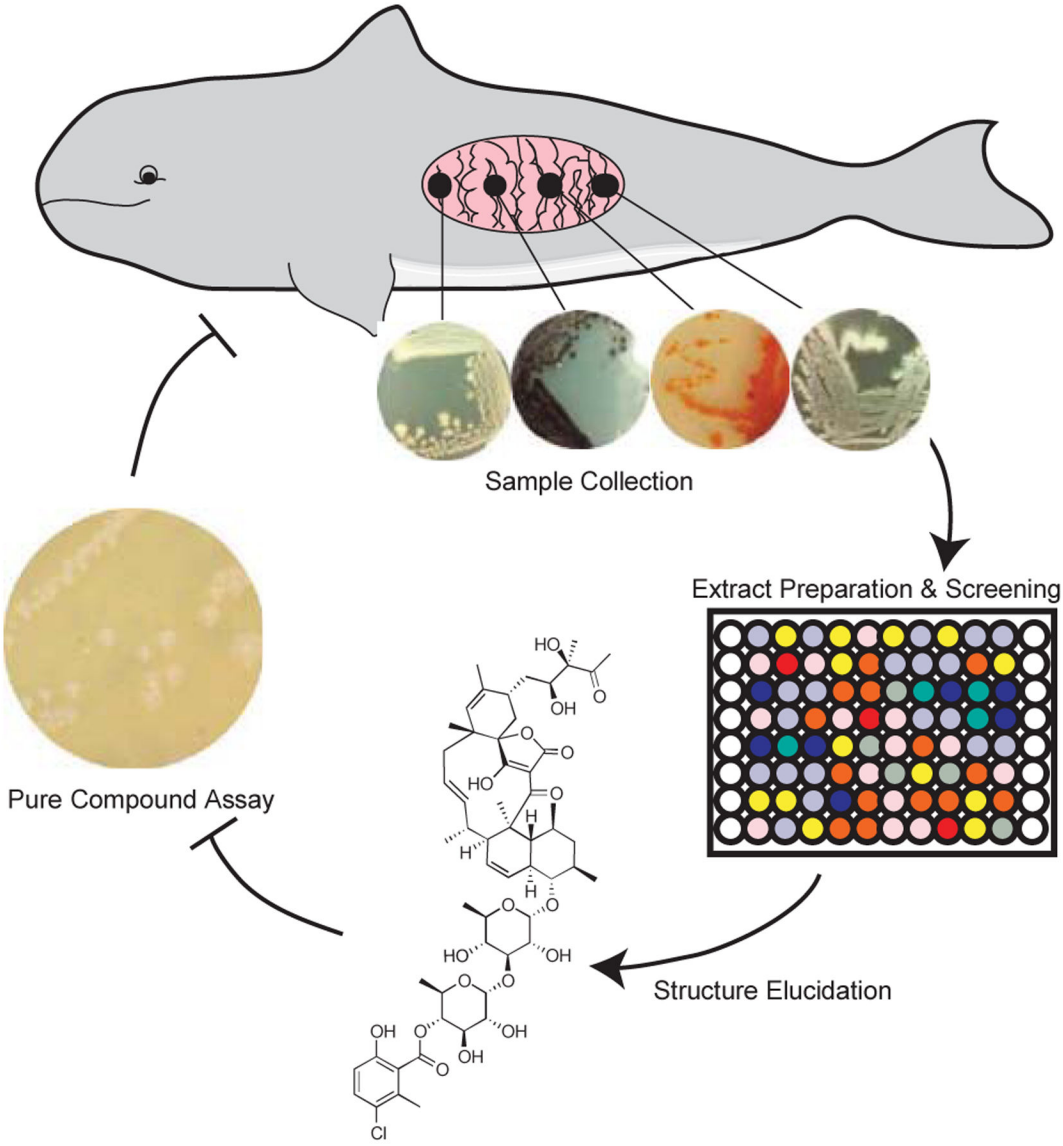

Fig. 1. Schematic of project workflow.

Isolates collected from marine mammal intestinal contents were fermented, and fractionated into 384 well plates for bioassays. Phocoenamicin was extracted from organism **MMA** 6B **HVS/10A** and analyzed as a pure compound.

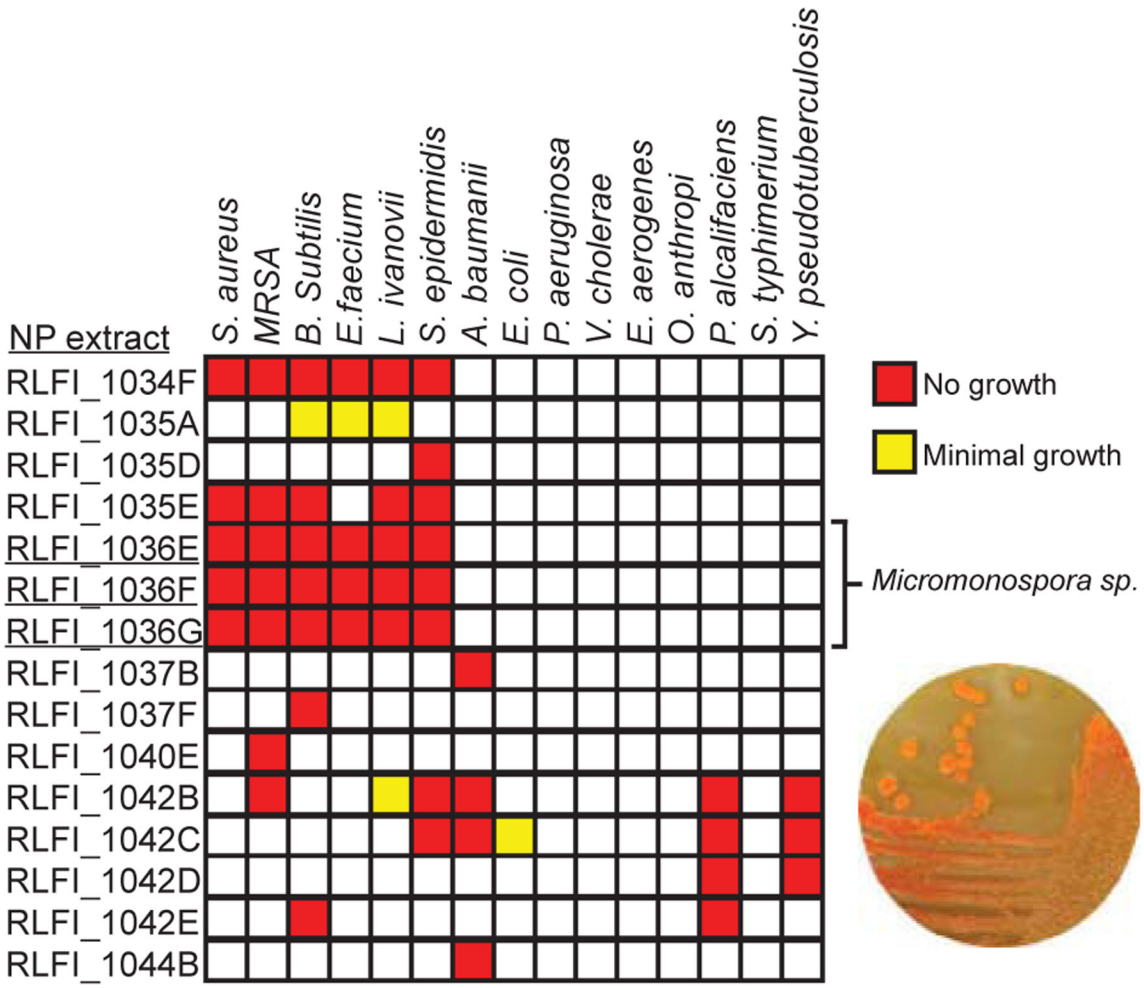

Fig. 2. Crude extract BioMAP dilution profiles illustrate potent activity against Gram-positive bacteria.

Natural product fractions on *y*-axis. Numbering denotes organism extract, RLFI denotes origin of organism, and letters A-G denote polarity of solvent used for extraction, red represents complete growth inhibition, yellow represents growth defects, white represents no growth inhibition.

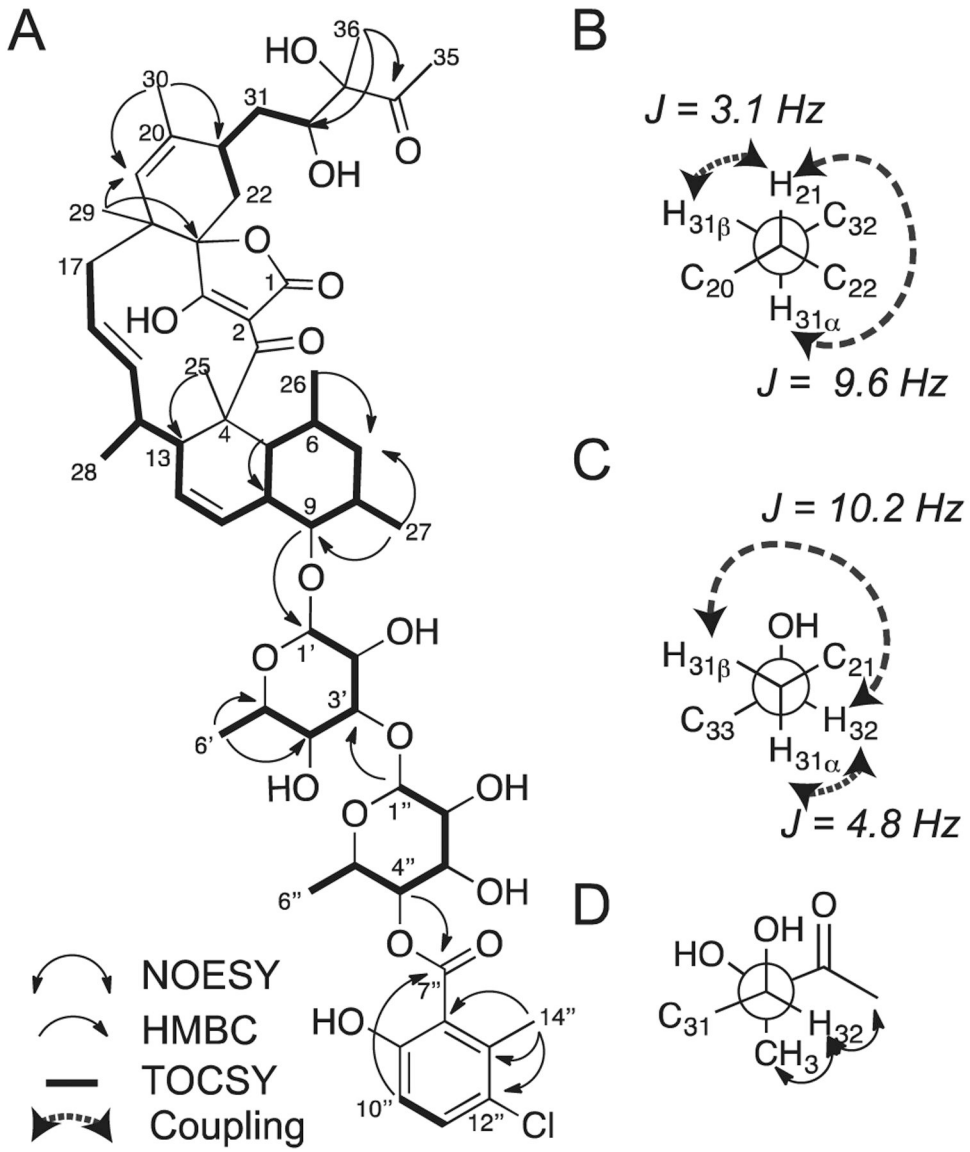

Fig. 3. Elucidation of phocoenamicin structure.

(A) Key NMR correlations used in the planar structure elucidation. (B) Newman projection along C_{21} (front) and C_{31} and key coupling constant values to determine bond angle. (C) Newman projection along C_{31} (front) and C_{32} and key coupling constant values. (D) Newman projection along C_{32} and C_{33} and NOE correlations.

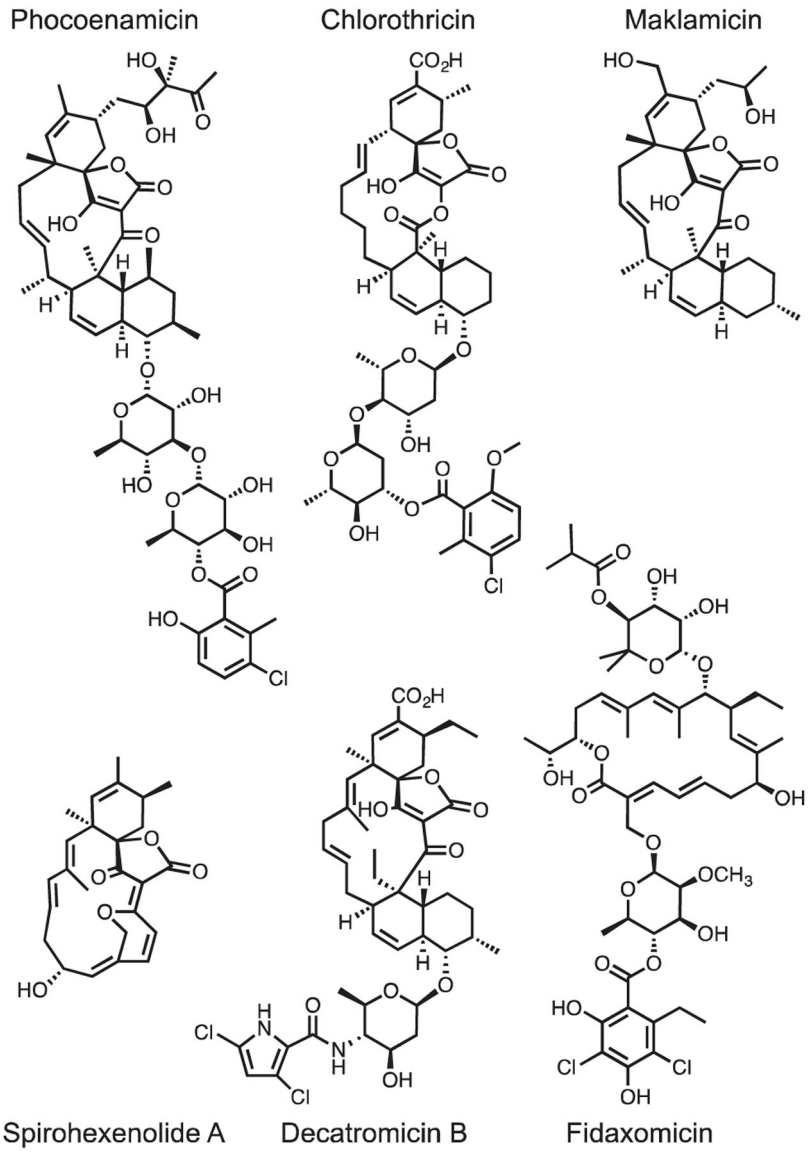

Fig. 4. Chemical Structures of phocoenamicin, relevant spirotetronates and fidaxomicin.

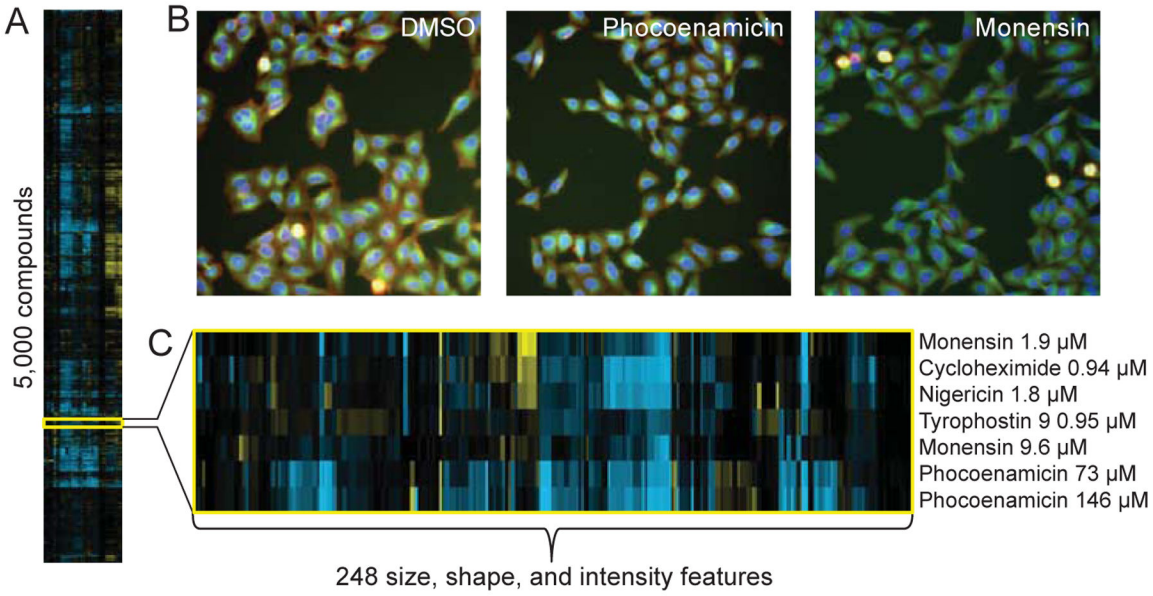

Fig. 5. Cytological profiling reveals clustering of phocoenamicin with ionophores.

(A) Hierarchical clustering of 5,000 compound treated wells evaluated against 248 cellular features. Positive and negative deviations relative to DMSO controls represented in yellow and blue, respectively. (B) Fluorescence images of drug-treated wells (phocoenamicin 146 μM, monensin 9.6 μM). Tubulin is represented in green, mitotic cells in cyan, actin in red, and DNA in blue. (C) Expanded fingerprints of phocoenamicin and neighboring cluster, which is enriched for ionophores.

Table 1.

Pure compound average MIC values.

All assays were run in triplicate. Abbreviations used: phocoenamicin (phoc.), vancomycin (vanc.), and rifampicin (rif.).

Organism	Phoc. (μM)	Vane. (μM)	Rif. (μM)
E. coli	>66	>66	8.3
P. aeruginosa	>66	>66	50
B. subtilis	2.8	0.15	0.12
E. faecium	11	3.6	4.47
S. aureus (MSSA)	1.0	0.69	0.010
S. aureus (MRSA)	1.0	0.87	0.0081
S. epidermidis	19	20	0.020
P. alcalifaciens	>66	>66	17
0. anthropi	>66	>66	22
E. aerogenes	>66	>66	17
A. baumanii	>66	>66	6.9
V. cholerae	>66	>66	28
S. typhimurium	>66	>66	33
Y. pseudotuberculosis	>66	>66	8.3
C. difficile	2.6	2.9	—